Lattice Boltzmann simulations of liquid-gas and binary fluid systems

Michael R. Swift, E. Orlandini, W. R. Osborn, and J. M. Yeomans
Theoretical Physics, Oxford University, 1 Keble Road, Oxford OX1 3NP, United Kingdom
(Received 25 January 1996)

We present the details of a lattice Boltzmann approach to phase separation in nonideal one- and two-component fluids. The collision rules are chosen such that the equilibrium state corresponds to an input free energy and the bulk flow is governed by the continuity, Navier-Stokes, and, for the binary fluid, a convection-diffusion equation. Numerical results are compared to simple analytic predictions to confirm that the equilibrium state is indeed thermodynamically consistent and that the kinetics of the approach to equilibrium lie within the expected universality classes. The approach is compared to other lattice Boltzmann simulations of nonideal systems. [S1063-651X(96)03211-4]

PACS number(s): 47.11.+j, 83.10.Lk, 05.70.Fh

I. INTRODUCTION

Our aim in this paper is to present the details of a lattice Boltzmann approach to modeling phase separation and flow in one- and two-component fluids. Possible applications of the method are numerous, ranging from questions of purely theoretical interest to those of industrial applicability. Examples include the effect of confinement and flow on phase separation, multiphase flow in porous media, the dynamics of complex fluids, and theoretical investigations of Boltzmann-like approaches to phase separation and out-of-equilibrium thermodynamics.

The lattice Boltzmann technique may arguably be classified as a mesoscopic approach to the simulation of fluid dynamics [1,2]. It is useful to consider it as lying between molecular dynamics, which accesses microscopic length scales, but as a result suffers from severe time constraints in the investigation of hydrodynamics, and finite-difference solutions of the Navier-Stokes equations, which contain no obvious physical input.

The genesis of the approach lies in the application of cellular automata to model fluid flow. In a seminal paper Frisch, Hasslacher, and Pomeau [3] showed that a cellular automaton model with collision rules that locally conserve mass and momentum could be used to model the Navier-Stokes equations in the continuum limit. In practical applications of this approach, however, fluctuations led to noisy data. Therefore Higuera, Succi, and Benzi [4] introduced the lattice Boltzmann method, which can be considered as a coarse-grained cellular automaton in which continuous distribution functions at each lattice site replace the Boolean variables.

The lattice Boltzmann approach has been shown to give convincing results for one-component flow [1]. It is particularly useful for simulating flows in complex geometries because of the relative ease of implementing tortuous boundary conditions (although care must be taken as to the detailed effect of the boundaries on the flow [5]). It has also been applied to multiphase fluids with promising results for questions as diverse as the exponents associated with spinodal decomposition [6–8] and the relative permeabilities for two-phase flow in a porous medium as a function of the relative densities of the two fluids [9]. However, the methods for introducing phase separation have thus far been based upon either a phenomenological rewriting of the collision rules [10] or the introduction of an effective microscopic interaction [11–13]. The drawback of these schemes is that the system relaxes to an equilibrium state that cannnot be described thermodynamically.

Therefore it is our aim here to describe a lattice Boltzmann approach that in equilibrium reaches a state that can be associated with a free energy, corresponding pressure tensor, and, for the binary fluid, chemical potential [14]. The technique has the added advantage that, given a simple choice of input free energy, the properties of the steady state, such as the coexistence curve and interface profiles, can be calculated analytically and compared to the results of the simulations. Our approach is similar in spirit to the Cahn-Hilliard theory of phase transitions in binary alloys [16]: the correct choice of the collision rules ensures that the system evolves towards the minimum of an input, nonlocal free-energy functional. Macroscopic fluid flow is governed by the Navier-Stokes equations.

We consider phase separation in both one-component or liquid-gas systems and two-component or binary fluids. Evidence is presented that the simulations reproduce the expected result that at short-time scales the kinetics of phase separation lies in different universality classes corresponding to nonconserved and conserved order parameters, respectively [17].

We hope that this approach will provide a useful step towards the goal of defining a fully thermodynamically consistent lattice Boltzmann method. The inclusion of the energy flow and the identification of an H theorem are still needed to attain this goal. This point is discussed more fully at the end of the paper.

The paper is organized as follows. In Sec. II we describe a general framework by which lattice Boltzmann schemes can be defined for a given set of microscopic conservation laws. This is applied to a one-component fluid and a binary fluid in Secs. III and V, respectively. Details of the derivations of the fluid equations of motion from the lattice Boltzmann collision rules are postponed to the Appendices. Results for each system as typified by a van der Waals fluid and two ideal gases with a mutual interaction are presented in Secs. IV and VI, respectively. Section VII aims to compare the approach to modeling phase separation described here to

other methods in the literature. Our conclusion, together with a discussion of the successes and omissions of our approach, conclude the paper.

II. GENERAL FRAMEWORK

The starting point for lattice Boltzmann simulations is the evolution equation, discrete in space and time, for a set of distribution functions $\{f_i\}$ defined on a lattice of points $\vec{x}$ [1]. Each f_i is associated with a lattice vector $\vec{e}_i$. Taking for simplicity a single-time relaxation approximation [18], the evolution equation for a given f_i takes the form

$$f_i(\vec{x}+\vec{e}_i\Delta t,t+\Delta t)-f_i(\vec{x},t)=-\frac{1}{\tau}(f_i-f_i^0), \tag{1}$$

where Δt is the time step and τ the relaxation parameter. f_i^0 is an equilibrium distribution function, the choice of which determines the physics inherent in the simulation.

Physical quantities are defined as moments of f_i. For example, $n=\Sigma_i f_i$ is a density and $p_\alpha=\Sigma_i f_i e_{i\alpha}$ is a momentum. Subscripts $\alpha,\beta,\ldots$ will be used to represent Cartesian coordinates and, as usual, a summation over repeated indices is assumed.

The conservation laws that determine the physics are introduced by choosing f_i^0 such that the conserved moments of f_i are equal to the corresponding moments of f_i^0. For example, if $p_\alpha=\Sigma_i f_i^0 e_{i\alpha}$ taking the first moment of Eq. (1) indicates that p_α is a locally conserved quantity in the simulation.

To obtain the continuum differential equations mimicked by Eq. (1) we Taylor expand the left-hand side to give

$$-\frac{1}{\tau}(f_i-f_i^0)=\sum_{k=1}^{\infty}\frac{1}{k!}\Delta t^k(\partial_t+e_{i\alpha}\partial_\alpha)^k f_i, \tag{2}$$

for which Eq. (1) is the exact discretization. ∂_t and ∂_α denote differentiation with respect to t and x_α, respectively. This equation can be solved recursively by the method of successive approximation. Retaining terms to $O((\Delta t)^2)$, Eq. (2) becomes

$$-\frac{f_i-f_i^0}{\tau\Delta t}=(\partial_t+e_{i\alpha}\partial_\alpha)f_i^0-(\tau-1/2)\Delta t(\partial_t^2+2e_{i\alpha}\partial_t\partial_\alpha+e_{i\alpha}e_{i\beta}\partial_\alpha\partial_\beta)f_i^0+O((\Delta t)^2). \tag{3}$$

Taking moments of Eq. (3) with respect to $\vec{e}_i$ gives equations relating the time evolution of the moments of f_i to the derivatives of the higher moments of the equilibrium distribution function. By choosing a suitable definition for certain higher moments of f_i^0 a given set of differential equations describing the dynamics of the conserved quantities can be simulated.

III. THE ONE-COMPONENT NONIDEAL FLUID

We first apply this approach to the flow of a one-component, nonideal fluid [19]. The dynamics of the fluid can be described by a single distribution function obeying the lattice Boltzmann equation (1) [1,4]. The important physical variables are the density n and the fluid momentum $n\vec{u}$, which are related to the distribution function by

$$n=\sum_i f_i, \quad nu_\alpha=\sum_i f_i e_{i\alpha}. \tag{4}$$

Each of these quantities is locally conserved in any collision process that forces the zeroth and first moments of the equilibrium distribution function to take the form

$$\sum_i f_i^0=n, \quad \sum_i f_i^0 e_{i\alpha}=nu_\alpha. \tag{5}$$

The higher moments of f_i^0 must be chosen such that the resulting continuum equations correctly describe the hydrodynamics of a nonideal, one-component fluid. Defining the second moment as

$$\sum_i f_i^0 e_{i\alpha}e_{i\beta}=P_{\alpha\beta}+nu_\alpha u_\beta, \tag{6}$$

where $P_{\alpha\beta}$ is the pressure tensor, leads to the continuity equation for the fluid density

$$\partial_t n+\partial_\alpha(nu_\alpha)=0 \tag{7}$$

and a Navier-Stokes level equation for the fluid momentum

$$\partial_t(nu_\beta)+\partial_\alpha(nu_\alpha u_\beta)=-\partial_\beta p_0+\partial_\alpha(\nu\partial_\alpha nu_\beta)+\partial_\beta(\lambda(n)\partial_\alpha nu_\alpha)-\left(\tau-\frac{1}{2}\right)\times\frac{dp_0}{dn}\Delta t\partial_\alpha(u_\beta\partial_\alpha n+u_\alpha\partial_\beta n), \tag{8}$$

where the shear viscosity ν and the bulk viscosity λ are given by

$$\nu=\frac{2\tau-1}{8}(\Delta t)c^2, \quad \lambda(n)=\left(\tau-\frac{1}{2}\right)\Delta t\left(\frac{c^2}{2}-\frac{dp_0}{dn}\right). \tag{9}$$

The differential equations (7) and (8) follow from taking the zeroth and first moments, respectively, of Eq. (3), using the conditions (5) and (6) and making additional approximations about the relative sizes of certain terms. The final unusual term must be included as density gradients may not be small but in homogeneous regions the equation reduces to the classical, incompressible, Navier-Stokes equation. Details of the calculation are given in Appendix A.

The thermodynamic aspects of the model enter through the pressure tensor $P_{\alpha\beta}$. Following the Cahn-Hilliard description of nonequilibrium dynamics [16], we calculate this function from the *equilibrium* free energy of the fluid mixture. To test our approach it seems appropriate to choose a simple and well-understood nonideal system, the van der Waals fluid, for which the free-energy functional within a gradient-squared approximation is [14]

$$\Psi=\int d\vec{r}\left(\psi(T,n)+\frac{\kappa}{2}(\nabla n)^2\right), \tag{10}$$

where $\psi(T,n)$ is the bulk free-energy density at a temperature T

$$\psi(T,n)=nT\ln\left(\frac{n}{1-nb}\right)-an^2 \tag{11}$$

and the second term gives the free-energy contribution from density gradients in an inhomogeneous system. The pressure tensor is related to the free energy in the usual way [15]

$$P_{\alpha\beta}(\vec{r})=p(\vec{r})\delta_{\alpha\beta}+\kappa\frac{\partial n}{\partial x_\alpha}\frac{\partial n}{\partial x_\beta}, \tag{12}$$

with

$$p(\vec{r})=p_0-\kappa n\nabla^2 n-\frac{\kappa}{2}|\vec{\nabla}n|^2, \tag{13}$$

where $p_0=n\psi'(n)-\psi(n)$ is the equation of state of the fluid.

Finally, to perform the simulation we need an explicit expression for f_i^0. For simplicitly we shall work on a triangular lattice taking six distribution functions f_i corresponding to the nearest-neighbor lattice vectors $e_i=c(\pm1,0),c(\pm1/2,\pm\sqrt{3}/2)$, which have the properties

$$\sum_i e_{i\alpha}=0,\quad \sum_i e_{i\alpha}e_{i\beta}=3c^2\delta_{\alpha\beta},$$

$$\sum_i e_{i\alpha}e_{i\beta}e_{i\gamma}=0,$$

$$\sum_i e_{i\alpha}e_{i\beta}e_{i\gamma}e_{i\delta}=\frac{3c^4}{4}(\delta_{\alpha\beta}\delta_{\gamma\delta}+\delta_{\gamma\beta}\delta_{\alpha\delta}+\delta_{\delta\beta}\delta_{\gamma\alpha}). \tag{14}$$

It will also be necessary to include a distribution function f_0 for rest particles with $\vec{e}_0=0$ in the simulation.

To satisfy the conditions on the first three moments of the equilibrium distribution function [Eqs. (5) and (6)], an expansion of the f_i^0 to second order in $\vec{u}$ is sufficient. We write

$$f_i^0=A+Bu_\alpha e_{i\alpha}+Cu^2+Du_\alpha u_\beta e_{i\alpha}e_{i\beta}+G_{\alpha\beta}e_{i\alpha}e_{i\beta} \tag{15}$$

and for the rest particles

$$f_0^0=A_0+C_0u^2, \tag{16}$$

where the coefficients $A,A_0,B,\ldots$ in the expansions depend on n and its derivatives. Using the relations (14), a suitable choice of coefficients is

$$A_0=n-6A,\quad A=(p_0-\kappa n\nabla^2 n)/3c^2,$$

$$B=n/3c^2,\quad C=-n/6c^2,$$

$$C_0=-n/c^2,\quad D=2n/3c^4,$$

$$G_{xx}=-G_{yy}=\frac{\kappa}{3c^4}\left\{\left(\frac{\partial n}{\partial x}\right)^2-\left(\frac{\partial n}{\partial y}\right)^2\right\},$$

$$G_{xy}=\frac{2}{3c^4}\kappa\frac{\partial n}{\partial x}\frac{\partial n}{\partial y}. \tag{17}$$

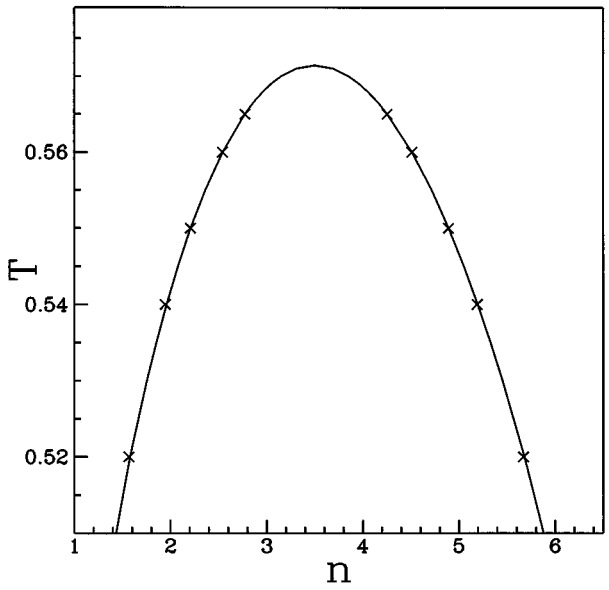

FIG. 1. Coexistence curve, temperature T versus density n for the van der Waals fluid. In the free energy (11) $a=9/49$ and $b=2/21$ corresponding to a critical density $n_c=7/2$ and a critical temperature $kT_c=4/7$. The solid line is the analytic result.

Examples of the choices of finite-difference approximations used to calculate the derivatives (which will affect correction terms in the simulations) are

$$\partial_\alpha n\approx\frac{1}{3c\Delta x}\sum_i n(\vec{r}+\vec{e}_i\Delta t)e_{i\alpha}, \tag{18}$$

$$\nabla^2 n\approx\frac{2}{3(\Delta x)^2}\left[\sum_i n(\vec{r}+\vec{e}_i\Delta t)-6n(\vec{r})\right]. \tag{19}$$

All the parameters are now in place to allow a numerical simulation of the lattice Boltzmann equation (1). This procedure in normally described in terms of two steps. The first of these is the collision step where each f_i relaxes to f_i^0 at a rate governed by τ. The second is a moving step where each $f_i(\vec{x})$ is moved to $f_i(\vec{x}+\vec{e}_i)$.

The explicit spatial discretization Δx in Eqs. (18) and (19) can be absorbed into the definition of κ. There are thus three free parameters c,κ, and τ that control the temporal and spatial scaling and the viscosity. By monitoring the growth of density variations, we have verified numerically that the scaling implied by Eqs. (8), (9), (12), and (13) holds for a wide range of control parameters.

IV. RESULTS FOR THE ONE-COMPONENT FLUID

We now present results for the one-component fluid. We confirm that the fluid behaves as expected in equilibrium, explore the universality class of the kinetics, but demonstrate that there are problems with Galilean invariance. Figure 1 shows the coexistence curve for $a=9/49$ and $b=2/21$, corresponding to a critical density $n_c=7/2$ and a critical tem-

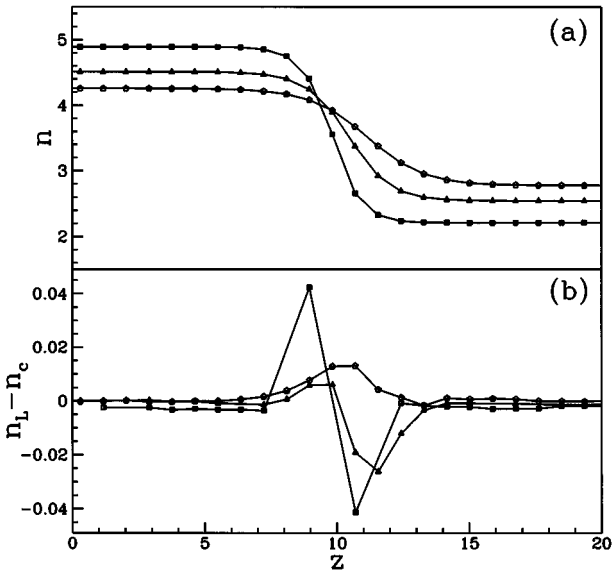

FIG. 2. (a) Equilibrium density profiles normal to a flat interface for a van der Waals fluid. n is the density and z the position on the lattice measured normal to the interface. The parameter values are $a=9/49$, $b=2/21$, $\kappa=0.01$, and $T=0.55,0.56$, and 0.57. The solid lines are numerical solutions of the continuum thermodynamic equations. (b) Difference between the results of the lattice Boltzmann simulations (n_L) and those (essentially exact) for the continuum model (n_C).

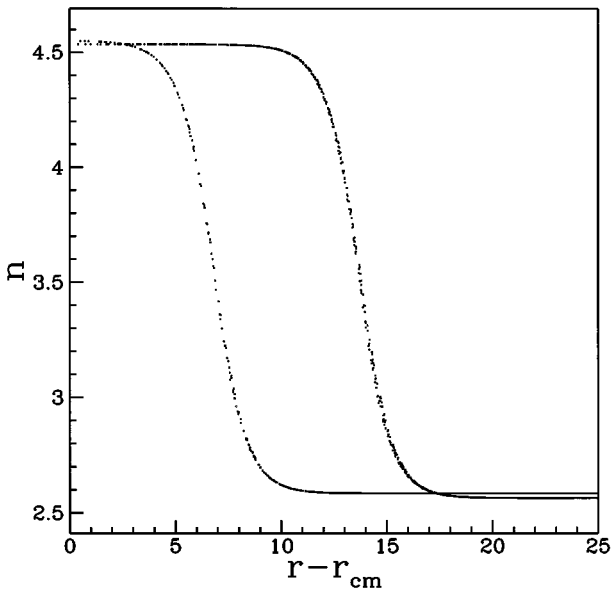

FIG. 3. Density n of equilibrated droplets plotted as the distance from the center of mass of the droplet $r-r_{\mathrm{c.m.}}$. The points lie on a single curve for each droplet, showing that any anisotropy in the droplet shape is very small. These simulations were run for $a=9/49$, $b=2/21$, and $\kappa=0.01$.

perature $T_c=4/7$. The points were obtained by equilibrating a flat interface between the liquid and gas phases for different temperatures and observing the maximum and minimum densities. Typically simulations were carried out on lattices of size 128×128 and allowed to equilibriate for 10^4 time steps. The line is the analytic result obtained from a Maxwell construction for the free energy (11). Good agreement is obtained over a wide range of density differences.

To demonstrate the extent to which the correct interfacial profile is reproduced, a planar interface, parallel to a lattice axis, was set up by relaxing a periodic density variation for $\sim10^4$ time steps. Figure 2(a) shows how the shape of the equilibrated interface varies with T. The solid lines are essentially exact numerical solutions for the interface profile of the continuum model described by the nonlocal free energy (10) and the data points represent the densities obtained from lattice Boltzmann simulations at lattice sites through the interface. Simulation parameters are given in the caption to Fig. 2. To provide a more transparent demonstration of the accuracy of the results the density difference between the lattice Boltzmann and continuum solutions is plotted in Fig. 2(b). Errors, which are a consequence of the discreteness of space and time, are less than 1%, becoming, as expected, larger as the interface becomes sharper. We note that interfaces of width ~2 lattice spacings can be obtained. Such narrow interfaces are useful in numerical simulations of, for example, domain growth where several domains are needed to give good statistics on a lattice of limited size.

To check the isotropy of the interface with respect to the lattice, circular droplets of diameters ~20 and ~30 lattice spacings were equilibriated for 10^4 time steps. The density was plotted as a function of the distance from the center of mass of the drops for all lattice points. The results, shown in Fig. 3, show no obvious anisotropy, which would be marked by some data points falling on different curves.

One of the problems experienced by both lattice Boltzmann and finite-difference simulations of interfaces is the existence of spurious, nonzero velocities in the interface region even in equilibrium. For the scheme described here they are zero for an interface parallel to a lattice direction, a fortuitous consequence of the imposition of the Maxwell construction. However, spurious velocities do exist for interfaces in other directions.

Evidence that these velocities are due to the finite space and time steps inherent in the simulation is presented in Fig. 4. This displays the maximum magnitude of the spurious velocity across the interface of an equilibrated circular droplet as a function of the relaxation parameter τ. There is a pronounced minimum close to the value $\tau^*=(1+1/\sqrt{3})/2$, where terms $O((\Delta t)^2)$ in the expansion (3) vanish. Note also that as κ is reduced and the interface becomes sharper the spurious velocities become greater as expected. A more detailed discussion of the dependence of the spurious velocities on the model parameters and a comparison of their magnitudes to those obtained in other lattice Boltzmann schemes for phase separation will be given elsewhere[20].

A useful check that the kinetics of the lattice Boltzmann scheme, that is, the way in which the system approaches equilibrium, lies within the expected universality class is provided by the rate of decay of an equilibrated interface [21,17]. An equilibrium interface was set up for an initial temperature $T_i<T_c$, where T_c is the critical temperature and the decay of the nonequilibrium surface tension

$$\sigma\propto\int\left(\frac{\partial n}{\partial z}\right)^2 dz, \tag{20}$$

where z is the coordinate perpendicular to the interface, was

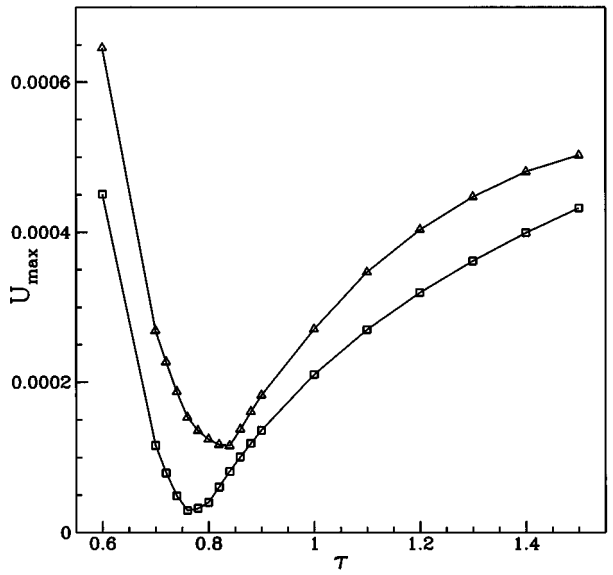

FIG. 4. Dependence of the spurious interface velocity on the relaxation parameter τ. There is a minimum near τ^* where terms $O[(\Delta t)^2]$ in expansion (3) vanish. $u_{\max}$ is the maximum value of the interface velocity for a circular equilibrated droplet. Results were obtained for $a=9/49$, $b=2/21$, $\kappa=0.01$ (triangles), and $\kappa=0.02$ (squares) coresponding to interfaces of widths ~ 5 and ~ 8 lattice spacings, respectively.

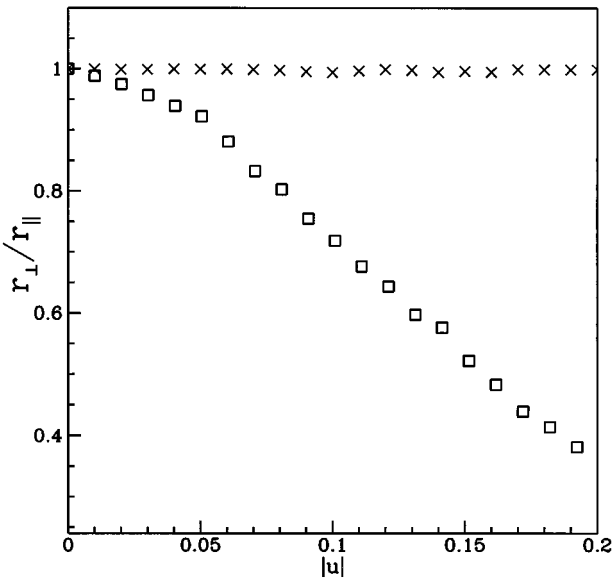

FIG. 5. Equilibrium droplet shape for a system moving with constant velocity $\vec{u}$ along a lattice direction. The droplet is elliptical and the ratio of the lengths of the minor to the major axe $r_\perp / r_\parallel$ is plotted. Results for the one-component fluid (squares) show large deviations from circular, resulting from a lack of Galilean invariance. For the binary fluid ($\times$) the droplet remains circular, showing that the system is very close to Galilean invariant.

measured following an instantaneous quench to final temperatures $T_f=T_c$ or $T_f>T_c$. The results are

$$\sigma\sim t^{-3/2}, \quad T_f=T_c; \quad \sigma\sim e^{-t}, \quad T_f>T_c, \tag{21}$$

consistent with the model A dynamics expected for a system with a nonconserved order parameter.

These values follow from a scaling argument. From the definition (20), $\sigma\sim n_0^2/L$, where L is the interface width and n_0 the value of the density far from the interface. For model A dynamics $L\sim t^{1/2}, T_f\geqslant T_c$. For very early times $n_0 \sim$ const, but these times are not accessible to the simulation. For later times $n_0\sim t^{-1/2}, T=T_c$ and $n_0\sim e^{-t}, T>T_c$, leading to the results (21). An important feature of these results is that they show that the lattice Boltzmann scheme described here gives sensible kinetics for temperatures $T\geqslant T_c$ as well as in the two-phase region.

We note that for later times hydrodynamic modes are expected to change the universality class of the fluid kinetics. These are not seen in a consideration of interface decay, but their effects have been observed in a simulation of domain growth [6].

In systems that phase separate, significant density gradients are created and this leads to measurable non-Galilean-invariant effects in the simulations. Note that the viscous terms in the Navier-Stokes equation (8) contain functions of the density within the first derivative and hence are not Galilean invariant.

To demonstrate the effect of the lack of Galilean invariance a circular droplet was brought to equilibrium and then a constant velocity $\vec{u}$ was imposed on the system. The droplet quickly came to rest.

A partial improvement follows if additional terms

$$\omega_1(u_\beta\partial_\alpha n+u_\alpha\partial_\beta n)+\omega_2 u_\gamma\partial_\gamma\delta_{\alpha\beta} \tag{22}$$

are added to the pressure tensor (6). By appropriate choice of ω_1 and ω_2 it is possible to remove some of the Galilean-invariant terms, but not all, as discussed in Appendix A. A moving droplet then deforms to a new equilibrium shape, an ellipse, with the ratio of the lengths of the minor and major axes decreasing with increasing flow velocity as shown in Fig. 5. An unphysical step in the velocity is seen across the interface.

V. A LATTICE BOLTZMANN SCHEME FOR BINARY FLUIDS

Our aim in this section is to describe how the lattice Boltzmann approach can be extended to describe the dynamics of binary fluids [22]. The main difference from the one-component case is that, as there are now two independent densities, two sets of lattice Boltzmann distribution functions $\{f_i\}$ and $\{g_i\}$ are now needed to correctly mirror the dynamics of the conserved quantities. These are taken to evolve according to the usual single relaxation-time lattice Boltzmann equation [see (1)][18]

$$f_i(\vec{x}+\vec{e}_i\Delta t,t+\Delta t)-f_i(\vec{x},t)=-\frac{1}{\tau_1}(f_i-f_i^0), \tag{23}$$

$$g_i(\vec{x}+\vec{e}_i\Delta t,t+\Delta t)-g_i(\vec{x},t)=-\frac{1}{\tau_2}(g_i-g_i^0). \tag{24}$$

A convenient choice of physical variables is the total fluid density n, the mean fluid velocity $\vec{u}$, and the density difference between the two fluid components $\Delta n=n_1-n_2$, where

n_1 and n_2 are the individual component densities. The physical variables are related to the distribution functions by

$$n=\sum_i f_i, \quad nu_\alpha=\sum_i f_i e_{i\alpha}, \tag{25}$$

$$\Delta n=\sum_i g_i. \tag{26}$$

These three quantities are locally conserved in any collision giving three constraints on the equilibrium distribution functions

$$\sum_i f_i^0=n, \quad \sum_i f_i^0 e_{i\alpha}=nu_\alpha, \tag{27}$$

$$\sum_i g_i^0=\Delta n. \tag{28}$$

The higher moments of f_i^0 and g_i^0 are defined so that the resulting continuum equations describe the dynamics of a binary liquid mixture. A suitable choice is

$$\sum_i f_i^0 e_{i\alpha}e_{i\beta}=P_{\alpha\beta}+nu_\alpha u_\beta, \tag{29}$$

$$\sum_i g_i^0 e_{i\alpha}=\Delta nu_\alpha, \tag{30}$$

$$\sum_i g_i^0 e_{i\alpha}e_{i\beta}=\Gamma\Delta\mu\,\delta_{\alpha\beta}+\Delta nu_\alpha u_\beta, \tag{31}$$

where $P_{\alpha\beta}$ is the pressure tensor, $\Delta\mu$ is the chemical potential difference between the two components, and Γ is a mobility.

This leads $O((\Delta t)^2)$ to the continuity equation for the total density

$$\partial_t n+\partial_\alpha(nu_\alpha)=0, \tag{32}$$

the Navier-Stokes equation for the mean fluid momentum

$$\partial_t(nu_\beta)+\partial_\alpha(nu_\alpha u_\beta)=-\partial_\beta p_0+\nu\nabla^2(nu_\beta) +\partial_\beta\{\lambda(n)\partial_\alpha(nu_\alpha)\}, \tag{33}$$

and a convection-diffusion equation for the density difference

$$\partial_t\Delta n+\partial_\alpha(\Delta nu_\alpha)=\Gamma\theta\nabla^2\Delta\mu-\theta\partial_\alpha\left(\frac{\Delta n}{n}\partial_\beta P_{\alpha\beta}\right). \tag{34}$$

The parameters in these equations are given by

$$\theta=(\Delta t)(\tau_2-1/2), \quad \nu=\frac{(2\tau_1-1)}{8}(\Delta t)c^2,$$

$$\lambda(n)=\left(\tau_1-\frac{1}{2}\right)\Delta t\left(\frac{c^2}{2}-\frac{dp_0}{dn}\right). \tag{35}$$

Their derivation from the expansion (3) is detailed in Appendix B.

Following the route for the one-component fluid in Sec. II, we now describe the thermodynamic aspects of the model that here are manifest through both $P_{\alpha\beta}$ and $\Delta\mu$. We choose the simplest model of a binary liquid: two ideal gases with a repulsive interaction energy that corresponds to the free-energy functional

$$\Psi=\int d\vec{r}\left(\psi(T,n,\Delta n)+\frac{\kappa}{2}(\nabla n)^2+\frac{\kappa}{2}(\nabla\Delta n)^2\right). \tag{36}$$

The bulk free-energy density at a temperature T is

$$\psi(\Delta n,n,T)=\frac{\lambda}{4}n\left(1-\frac{\Delta n^2}{n^2}\right)-Tn+\frac{T}{2}(n+\Delta n)\ln\left(\frac{n+\Delta n}{2}\right) +\frac{T}{2}(n-\Delta n)\ln\left(\frac{n-\Delta n}{2}\right), \tag{37}$$

where λ measures the strength of the interaction. For $T<T_c=\frac{1}{2}\lambda$ the bulk system phase separates into one of two phases, with density differences $\pm\Delta n$. The chemical potential difference and pressure tensor follow from the free energy in the usual way [23],

$$\Delta\mu(\Delta n,n,T)=-\frac{\lambda}{2}\frac{\Delta n}{n}+\frac{T}{2}\ln\left(\frac{1+\Delta n/n}{1-\Delta n/n}\right)-\kappa\nabla^2(\Delta n), \tag{38}$$

$$P_{\alpha\beta}(\vec{r})=p(\vec{r})\delta_{\alpha\beta}+\kappa\frac{\partial n}{\partial x_\alpha}\frac{\partial n}{\partial x_\beta}+\kappa\frac{\partial\Delta n}{\partial x_\alpha}\frac{\partial\Delta n}{\partial x_\beta}, \tag{39}$$

where

$$p(\vec{r})=nT-\kappa(n\nabla^2 n+\Delta n\nabla^2\Delta n)-\frac{\kappa}{2}(|\nabla n|^2+|\nabla\Delta n|^2). \tag{40}$$

Finally, we present explicit expressions for f_i^0 and g_i^0. Working, as for the one-component fluid, on a triangular lattice, we define

$$f_i^0=A+Bu_\alpha e_{i\alpha}+Cu^2+Du_\alpha u_\beta e_{i\alpha}e_{i\beta}+G_{\alpha\beta}e_{i\alpha}e_{i\beta}, \tag{41}$$

$$f_0^0=A_0+C_0u^2, \tag{42}$$

$$g_i^0=H+Ku_\alpha e_{i\alpha}+Ju^2+Qu_\alpha u_\beta e_{i\alpha}e_{i\beta}, \tag{43}$$

$$g_0^0=H_0+J_0u^2. \tag{44}$$

A suitable choice of the coefficients in these expansions, consistent with Eqs. (27)–(31), is

$$A_0=n-6A, \quad A=(p_0-\kappa\Delta n\nabla^2\Delta n-\kappa n\nabla^2 n)3c^2,$$

$$B=n/3c^2, \quad C=-n/6c^2, \quad C_0=-n/c^2, \quad D=2n/3c^4,$$

$$G_{xx}=-G_{yy}=\frac{\kappa}{3c^4}\left\{\left(\frac{\partial n}{\partial x}\right)^2-\left(\frac{\partial n}{\partial y}\right)^2\right\} +\frac{\kappa}{3c^4}\left\{\left(\frac{\partial\Delta n}{\partial x}\right)^2-\left(\frac{\partial\Delta n}{\partial y}\right)^2\right\},$$

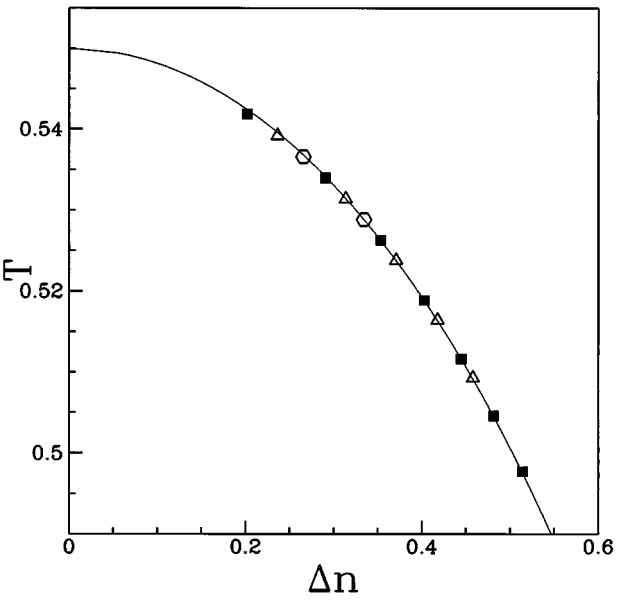

FIG. 6. Coexistence curve, the relation between the density difference between the two phases Δn and the temperature T, for the binary fluid defined by the equation of state (37) for $\lambda=1.1$ corresponding to $T_C=0.55$. Different symbols denote simulations run at different uniform fluid velocities: $\vec{u}=0.0$ (filled squares), $\vec{u}=0.1$ (triangles), $\vec{u}=0.2$ (hexagons). The solid line is the exact result.

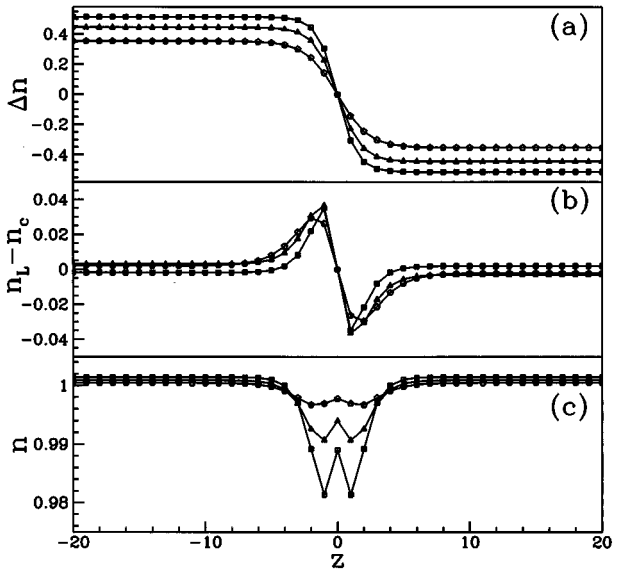

FIG. 7. (a) Equilibrium density profiles normal to a flat interface for the binary fluid defined by the free energy (10) with $\lambda=1.1$. Δn is the density difference between the two phases and z the position on the lattice measured normal to the interface. Results are given for $\kappa=0.01$ and $T=0.498$, 0.511, and 0.526. (b) Difference between the results of the lattice Boltzmann simulations (n_L) and exact results for the continuum model (n_C). (c) Variation of the density n across the interface.

$$G_{xy}=\frac{2}{3c^4}\kappa\left[\frac{\partial n}{\partial x}\frac{\partial n}{\partial y}+\frac{\partial \Delta n}{\partial x}\frac{\partial \Delta n}{\partial y}\right],$$

$$H_0=\Delta n-6H,\quad H=\frac{\Gamma\Delta\mu}{3c^2},\quad K=\frac{\Delta n}{3c^2},\quad J=-\frac{\Delta n}{6c^2},$$

$$J_0=-\Delta n/c^2,\quad Q=\frac{2\Delta n}{3c^4}. \tag{45}$$

VI. RESULTS FOR A BINARY FLUID

Here we detail the results of simulations on the binary fluid mixture. To check that the expected equilibrium is obtained we measured the coexistence curve for $\lambda=1.1$ corresponding to $kT_c=0.55$. The results, typically obtained from runs on lattices of size 128×128 equilibrated for 5×10^4 time steps, are shown in Fig. 6. The exact coexistence curve, which can be calculated from the free energy (37), is given for comparison. Similar measurements taken when the system was moving at a constant velocity, which provide a check on the Galilean invariance of the model, are also shown and will be discussed below.

The profiles of a flat interface parallel to a lattice axis for the same value of λ and different temperatures are displayed in Fig. 7(a). Figure 7(b) shows the deviations of the density profiles from the exact continuum results, which follow from the nonlocal free energy (36). These results suggest that discreteness errors in the simulations $\sim$1–2%. Figure 7(c) shows the total density across the interface, which is approximately constant.

Another important check concerns the isotropy of the interface profile with respect to the lattice. Circular domains of the phase with $\Delta n>0$ within the phase with $\Delta n<0$ were brought to equilibrium. Figure 8 displays Δn at all lattice points as a function of the distance from the point at which the first moment of Δn is zero for each droplet. There is no evidence that any data points lie on different curves, thus showing that the droplets are at least very close to isotropic.

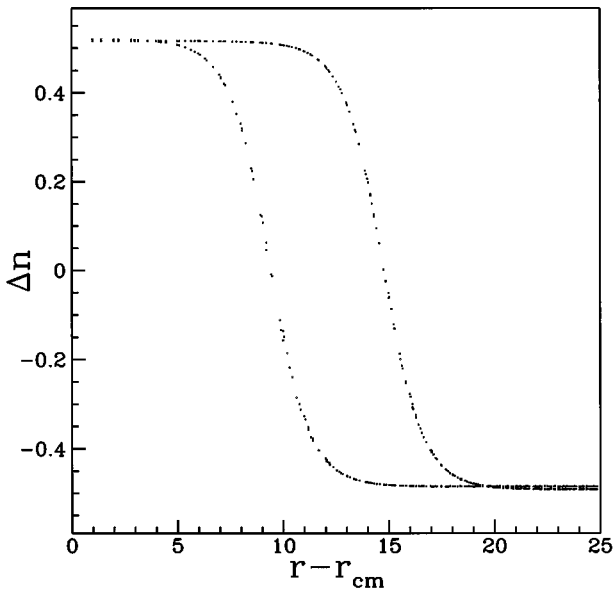

FIG. 8. Order parameter Δn of equilibrated droplets plotted as the distance from the center of mass of the droplet $r-r_{\mathrm{c.m.}}$. The points lie on a single curve for each droplet showing that any anisotropy in the droplet shape is very small. These simulations were run for $\lambda=1.1$, $\kappa=0.2$, and $T=0.5$.

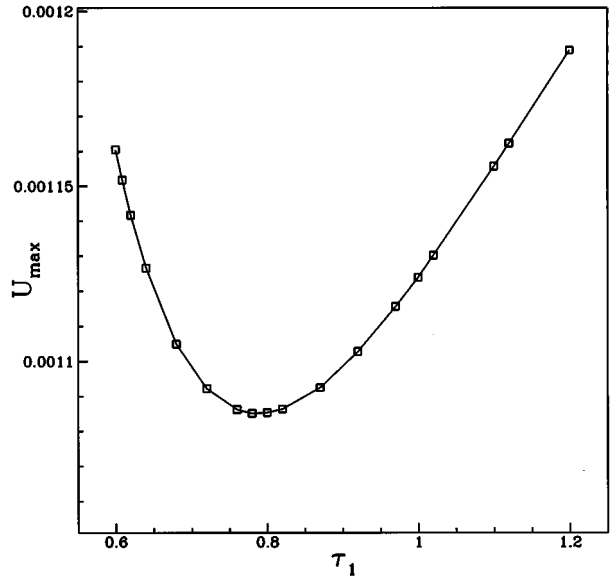

FIG. 9. Dependence of the spurious interface velocity on the relaxation parameter τ. There is a minimum near τ^* where terms $O((\Delta t)^2)$ in the expansion (3) vanish. $u_{\max}$ is the maximum value of the interface velocity for a circular equilibrated droplet. Results were obtained for $\lambda=1.1$, $\kappa=0.2$, and $T=0.5$ corresponding to an interface of width ~ 5 lattice spacings.

Just as for the one-component fluid, discreteness errors in the simulation lead to spurious velocities in equilibrium in the interface region for the binary fluid. An example of these is plotted in Fig. 9. Again, there is a pronounced minimum near $\tau_1=\tau^*$ where terms $O((\Delta t)^2)$ disappear from the expansion (3). For a flat interface parallel to a lattice axis there are no spurious velocities.

It is interesting to compare results for the decay of an equilibrated interface following an instantaneous increase in temperature to $T_f=T_c$ or $T_f>T_c$ to those for a one-component fluid [21]. They are expected to differ because the binary fluid has a conserved order parameter. This means that it lies in the model B universality class in the regime when hydrodynamics is unimportant [17].

The nonequilibrium surface tension

$$\sigma \propto \int \left(\frac{\partial(\Delta n)}{\partial z} \right)^2 dz \tag{46}$$

was measured and was found to decay with time as

$$\sigma \sim t^{-1/4}, \quad T_f=T_c; \quad \sigma \sim t^{-1/2}, \quad T_f>T_c. \tag{47}$$

These results should be compared to those for the liquid gas system (21).

The values are again in agreement with a simple scaling argument. From (46) $\sigma \sim (\Delta n_0)^2/L$, where L is the interface width and Δn_0 the value of the density difference far from the interface. For model B dynamics $\Delta n_0 \sim$ const; $L \sim t^{1/2}$, $T>T_c$; and $L \sim t^{1/4}$, $T=T_c$, leading immediately to (47). This provides a very clean and simple numerical test that our model does indeed lie within the model B universality class.

The lack of Galilean invariance for the one-component fluid does not occur for the binary fluid simulations. This is because, in the latter case, the density is essentially constant throughout the fluid. To demonstrate this the coexistence curve was measured for systems moving at a constant bulk velocity. The results, plotted in Fig. 6, show no velocity dependence. A second set of results, which highlights the difference between the one- and two-component fluids is shown in Fig. 5. The deformation of an originally circular droplet in a fluid moving with constant velocity seen in the former case does not occur for the latter. However, we note that the problem will reappear if the two components of the binary fluid have different masses [24].

VII. COMPARISON TO OTHER LATTICE BOLTZMANN SCHEMES OF PHASE SEPARATION

We now compare our approach to other lattice Boltzmann schemes for phase separation appearing in the literature. A scheme for modeling immiscible binary mixtures, which has been widely used, was introduced for cellular automata by Rothman and Keller [25] and extended to the lattice Boltzmann framework by Gunstensen *et al.* [10]. The Gunstensen *et al.* scheme induces phase separation by a phenomenological rewriting of the collision rules. It can be described within the framework of a Bhatnagar-Gross-Krook approximation [18] in two steps.

In the first step the distribution function for the total density $\{f_i\}$ is updated as usual [Eq. (23)] *but* with an equilibrium distribution f_i^0 corresponding to an ideal gas. A color gradient is then defined at each node

$$q_\alpha(\vec{r}) = \sum_i e_{i\alpha}\{n_r(\vec{r}+\vec{e}_i) - n_b(\vec{r}+\vec{e}_i)\} \approx 3c^2 \partial_\alpha \Delta n, \tag{48}$$

where $n_r=(n+\Delta n)/2$ and $n_b=(n-\Delta n)/2$ are the densities of the two species. An extra term

$$\beta_1 |\vec{q}| \cos 2\phi_i, \tag{49}$$

where

$$\cos\phi_i = \frac{\vec{q}\cdot\vec{e}_i}{|\vec{q}||\vec{e}_i|} \tag{50}$$

is added to $\{f_i\}$.

Writing

$$\cos 2\phi_i = 2\cos^2\phi_i - 1 = 2\frac{q_\alpha q_\beta e_{i\alpha} e_{i\beta}}{|\vec{q}|^2 c^2} - 1, \tag{51}$$

it is apparent that the initial updating, together with the addition of the extra term (49), is equivalent to a single updating, but with a redefined equilibrium distribution function

$$\overline{f_i^0} = \overline{A} + B e_{i\alpha} u_\alpha + C u^2 + D u_\alpha u_\beta e_{i\alpha} e_{i\beta} + \overline{G}_{\alpha\beta} e_{i\alpha} e_{i\beta}. \tag{52}$$

The coefficients B,C,D (and those appearing in f_0^0) are identical to those defined in Eq. (45). However, differences appear in

$$\overline{A}=n/3-\beta_1\tau|\vec{q}|,$$

$$\overline{G_{xx}}=\frac{2\beta_1\tau}{c^2|\vec{q}|}q_x^2,\quad \overline{G_{yy}}=\frac{2\beta_1\tau}{c^2|\vec{q}|}q_y^2,\quad \overline{G_{xy}}=\frac{2\beta_1\tau}{c^2|\vec{q}|}q_xq_y. \tag{53}$$

These coefficients correspond to the definitions of the moments of f_i^0 given in equations (27) and (29) if the pressure tensor is taken to be

$$\overline{P_{\alpha\beta}}=\overline{p(\vec{r})}\,\delta_{\alpha\beta}+\frac{3\beta_1}{|\vec{q}|}\tau c^2(3c^2)^2\partial_\alpha(\Delta n)\partial_\beta(\Delta n), \tag{54}$$

where

$$\overline{p(\vec{r})}=(n-\tfrac{3}{2}\beta_1\tau|\vec{q}|)c^2. \tag{55}$$

This form for the pressure tensor should be compared to Eqs. (39) and (40). The important term that gives rise to an energy associated with density gradients and hence to a surface tension $\overline{\kappa}=3\beta_1(3c^2)^2\tau c^2/|\vec{q}|$ is included in the Gunstensen *et al.* approach, but the lack of $\nabla^2\Delta n$ terms in the diagonal part of the pressure tensor indicates that there is no consistency with a free-energy functional.

In the second step of the Gunstensen *et al.* approach [10] the two densities n_r and n_b are redistributed so as to preserve a sharp interface. The prescription for this is to maximize the scalar product of the color gradient [Eq. (48)] and the color flux $\Sigma_i g_i\vec{e}_i$ at a site with the constraints that the f_i and the total densities of the two species remain constant.

The maximization step is carried out numerically precluding an analytic comparison to the approach described here. However, its effect is to leave $\Sigma g_i^0=\Delta n$, as in Eq. (28), but to introduce complicated additional terms into both $\Sigma g_i^0 e_{i\alpha}$ and $\Sigma g_i^0 e_{i\alpha}e_{i\beta}$, which presumably mimic the effect of the chemical potential. In the Gunstensen *et al.* approach the interfaces are sharp, but this appears not to affect the kinetics of domain growth [26]. An extension of the method that allows a phenomenological parameter that can be used to tune the interface width has been proposed by D'Ortona *et al.* [27].

A different approach to the introduction of phase separation has been proposed by Shan and Chen [11,12]. These authors base their development on the assumption that phase separation is driven by microscopic interactions between the lattice Boltzmann sites. The effect of the interactions is to introduce an additional *momentum* change at each iteration of the recursion equations.

Hence, for one-component fluids, the equation (5) for the first moment of the equilibrium distribution function is replaced by

$$\sum f_i^0 e_{i\alpha}=nu_\alpha-\tau G\psi(\vec{x})\sum_i \psi(\vec{x}+\vec{e}_i)e_{i\alpha}, \tag{56}$$

where G measures the strength of the interaction and ψ is a function of the density n. The second moment of the equilibrium distribution function is taken as equal to the pressure of an *ideal* gas, together with a streaming term [compare Eq. (6)].

These definitions for the moments of f^0 lead, in the usual way (see Appendix A), to a continuity equation, but with a spurious diffusive term

$$\partial_t n+\partial_\alpha nu_\alpha=\frac{3Gc^2}{2}\nabla^2\psi, \tag{57}$$

and to the Navier-Stokes equation with a nonideal equation of state

$$p_0=\frac{c^2}{2}\left[\frac{(1-d_0)n}{6}+3G\psi^2(n)\right], \tag{58}$$

where d_0 is a constant. Hence the system spontaneously phase separates with $-(1-d_0)/G$ behaving in a way akin to temperature.

The primary drawback of this approach is that the equilibrium state is not thermodynamically consistent and has no underlying free energy. This means that, in general, calculations of the properties of the system, for example, the surface tension, using a mechanic approach (i.e., from the pressure tensor) or a thermodynamic approach (i.e., from a Maxwell construction on the equation of state) are inconsistent. It would be interesting to ascertain whether this approach gives the correct kinetics for the approach to equilibrium by, say, following the decay of an interface equilibrated below T_c as the temperature is raised to $\geqslant T_c$ or whether the additional diffusive term in the continuity equation drives a crossover to a different universality class.

Shan and Doolen [13] have more recently given a detailed account of the application of this approach to miscible binary fluids. There is an extra momentum exchange between the components, introduced as an extra term in the definition of the first moment of the equilibrium distribution function Eq. (30). Given care in the identification of the macroscopic fluid velocity this leads to convection-diffusion equations for each component. The diffusion is driven by the difference in the fluid densities from their equilibrium values and the diffusion coefficients are a complicated function of the fluid concentrations and the parameters appearing in the interaction terms.

We emphasize that in the approach described in this paper phase separation is driven by terms in the second moments of the equilibrium distribution functions, whereas in the Shan-Chen-Doolen method the additional terms appear in the first moments. Although one might argue that considering microscopic interactions naturally leads to momentum changes it is far from obvious that the lattice Boltzmann sites should be viewed as microscopic entities. Regarding the simulation as mesoscopic, the effect of interactions are more physically input as corrections to thermodynamic variables such as the pressure tensor. This approach has the advantage of no spurious diffusion term in the equation for one-component flow, a thermodynamically consistent equilibrium state, and a much simpler diffusion equation for binary flow.

As far as we are aware the only other scheme in the literature that relies on corrections to the second moment of the distribution function is a lattice Boltzmann scheme for miscible fluids due to Flekkøy [28]. The main difference between his approach and that presented here is that Eq. (31),

which defines the second moment of the distribution function for the density difference, is replaced by

$$\sum_i g_i^0 e_{i\alpha} e_{i\beta} = \Delta n \, \delta_{\alpha\beta}/2. \tag{59}$$

This, together with the assumptions that $P_{\alpha\beta} = \frac{1}{2} n \delta_{\alpha\beta}$ and that the density is constant, leads to a diffusion equation (rewritten in the notation of this paper)

$$\partial_t \Delta n + u_\alpha \partial_\alpha \Delta n = (\tau - 1/2)\Delta t \{\nabla^2 \Delta n/2 - u_\alpha u_\beta \partial_\alpha \partial_\beta \Delta n\}. \tag{60}$$

A difference between this and equation (34) is the appearance of the non-Galilean-invariant term on the right-hand side of (60). This gives a velocity dependence to the diffusion coefficient that can be removed by adding $\Delta n u_\alpha u_\beta$ to the right-hand side of the definition (59). A more physical difference is that the diffusion is driven by the density difference Δn rather than the chemical potential difference $\Delta \mu$. Hence the simulation will be unstable in the immiscible regime.

VIII. DISCUSSION

In this paper we have described a lattice Boltzmann scheme for the simulation of phase separation and flow in one- and two-component fluids. The main different feature of the approach is that in equilibrium the system is described by a chosen free energy. Hence mechanical and thermodynamic calculations of physical properties are, by construction, consistent in the steady state. The approach to equilibrium is governed by the input free energy in a way similar in spirit to the Cahn-Hillard approach to phase separation in binary alloys. Bulk flow properties are described by the continuity and Navier-Stokes equations. For the binary fluid there is also a convection-diffusion equation for the density difference with the diffusion being controlled by the chemical potential difference between the two components.

Numerical results for the coexistence curve and interface profiles were shown to be in excellent agreement with the analytic calculations. Evidence presented here and elsewhere [6] indicates that the kinetics of phase separation at early times lies within the model *A* universality class for the one-component fluid for which the order parameter is not conserved and the model *B* universality class for the two-component fluid where it is. Moreover, the scheme has sensible kinetics above and at, as well as below, the critical temperature.

A problem is the lack of Galilean invariance, which occurs for the liquid-gas system because of variations in the density that appear inside derivatives in the Navier-Stokes equation. Although this can be alleviated by including additional terms in the pressure tensor Eq. (6), it cannot be removed. The continuum Boltzmann equation is, of course, Galilean invariant, and the invariance is lost in going to the lattice version. More work is needed to understand and overcome this shortcoming.

Still missing from the approach is a correct treatment of the flow of energy: a macroscopic differential equation describing energy conservation is needed. Although such an equation has been included in a lattice Boltzmann scheme for an ideal gas [29] it is far from obvious how to treat potential energy correctly. Moreover, on a microscopic level, an *H* theorem must be identified before a fully thermodynamically consistent scheme is possible. Perhaps one should emphasize that the Navier-Stokes equations themselves contain only the equation of state and are reproduced by virtually any method of driving phase separation that conserves momentum. The actual equilibrium obtained is determined by higher-order corrections in the simulation. A corollary is that to get energy flow correct, it will not only be necessary to simulate the correct macroscopic conservation equations but also to introduce the correct relations between the microscopic thermodynamic properties.

Another interesting direction for future research is the relationship between lattice Boltzmann and finite-difference approaches to the solution of the Navier-Stokes equations. That the two schemes are intimately related was pointed out by Ancona [30]. Recently Nadiga and Zaleski [31] have introduced the correct nonideal pressure tensor into a finite-difference simulation of the Navier-Stokes equations ensuring that a thermodynamically consistent equilibrium is obtained.

ACKNOWLEDGMENTS

We would like to thank J. Banavar, B. Boghosian, P. Coveney, D. D'Humières, and S. Zaleski for interesting discussions. This work was supported by grants from the EPSRC and the European Community.

APPENDIX A

Our aim is to show how the continuity and Navier-Stokes equations for a one-component fluid follow from the single relaxation time lattice Boltzmann approximation Eq. (1). Our starting point is Eq. (3).

Summing both sides of Eq. (3) over i and using Eqs. (4) and (5) gives

$$0 = \partial_t n + \partial_\alpha (n u_\alpha) - (\tau - 1/2)\Delta t \left\{ \partial_t^2 n + 2 \partial_\alpha \partial_t (n u_\alpha) + \partial_\alpha \partial_\beta \sum_i f_i^0 e_{i\alpha} e_{i\beta} \right\} + O((\Delta t)^2). \tag{A1}$$

Multiplying Eq. (3) by $e_{i\beta}$ and summing over i gives

$$0 = \partial_t (n u_\beta) + \partial_\alpha \sum_i f_i^0 e_{i\alpha} e_{i\beta} - (\tau - 1/2)\Delta t \left\{ \partial_t^2 (n u_\beta) + 2 \partial_t \partial_\alpha \sum_i f_i^0 e_{i\alpha} e_{i\beta} + \partial_\alpha \partial_\gamma \sum_i f_i^0 e_{i\alpha} e_{i\beta} e_{i\gamma} \right\} + O((\Delta t)^2). \tag{A2}$$

From Eqs. (A1) and (A2), respectively,

$$\partial_t n = -\partial_\alpha (n u_\alpha) + O(\Delta t), \tag{A3}$$

$$\partial_t (n u_\beta) = -\partial_\alpha \sum_i f_i^0 e_{i\alpha} e_{i\beta} + O(\Delta t). \tag{A4}$$

Substituting these expressions into the curly brackets in Eq. (A1) shows that this term vanishes to this order and we are left with the continuity equation (7).

Similarly using Eq. (A4) shows that the first, together with half of the second, term in the curly brackets in Eq. (A2) can be neglected as higher order. We consider the remaining terms in (A2) in turn.

(i) Using the definition of the second moment of f_i^0, Eq. (6)

$$\partial_\alpha \sum_i f_i^0 e_{i\alpha} e_{i\beta} = \partial_\alpha P_{\alpha\beta} + \partial_\alpha (n u_\alpha u_\beta) \approx \partial_\beta p_0 + \partial_\alpha (n u_\alpha u_\beta) \tag{A5}$$

using (12) and neglecting higher-order derivatives.

(ii) Similarly,

$$\begin{aligned} \partial_t \partial_\alpha \sum_i f_i^0 e_{i\alpha} e_{i\beta} &= \partial_t \partial_\alpha (P_{\alpha\beta} + n u_\alpha u_\beta) \\ &\approx \partial_\alpha \partial_t p_0 + \partial_\alpha [u_\alpha \partial_t (n u_\beta) + n u_\beta \partial_t u_\alpha] \\ &\approx -\partial_\beta \frac{dp_0}{dn} \partial_\gamma (n u_\gamma) \\ &\quad - \partial_\alpha (u_\alpha \partial_\beta p_0 + u_\beta \partial_\alpha p_0), \end{aligned} \tag{A6}$$

again neglecting higher-order derivatives. The final step follows from using Eqs. (A3)–(A5).

(iii) Using the definition of f_i^0, Eq. (15), together with the property of the lattice vectors Eq. (14), the final term in curly brackets in Eq. (A2) may be rewritten as

$$\begin{aligned} \partial_\alpha \partial_\gamma \sum_i f_i^0 e_{i\alpha} e_{i\beta} e_{i\gamma} &= \frac{c^2}{4} \partial_\alpha \partial_\gamma (n u_\gamma \delta_{\alpha\beta} + n u_\beta \delta_{\alpha\gamma} + n u_\alpha \delta_{\beta\gamma}) \\ &= \frac{c^2}{4} [2 \partial_\beta \partial_\gamma (n u_\gamma) + \nabla^2 n u_\beta] \end{aligned} \tag{A7}$$

Substituting (A5)–(A7) back into (A2), one obtains the Navier-Stokes level equation (8).

The viscous terms in the momentum equation (8) are not Galilean invariant when density gradients are present. Some of the non-Galilean invariant terms can be removed by adding terms to the pressure tensor Eq. (6):

$$\begin{aligned} \sum_i f_i^{\mathrm{eq}} e_{i\alpha} e_{i\beta} &= P_{\alpha\beta} + n u_\alpha u_\beta + \omega_1 (u_\beta \partial_\alpha n + u_\alpha \partial_\beta n) \\ &\quad + \omega_2 u_\gamma \partial_\gamma n. \end{aligned} \tag{A8}$$

The Navier-Stokes level equation then becomes

$$\begin{aligned} \partial_t (n u_\beta) + \partial_\alpha (n u_\alpha u_\beta) &= -\partial_\beta p_0 + \nu \partial_\alpha (n \partial_\alpha u_\beta) + \partial_\beta (\lambda n \partial_\alpha u_\alpha) \\ &\quad + \partial_\alpha [(\nu - \omega_1 - \zeta) u_\beta \partial_\alpha n] \\ &\quad + \partial_\beta [(\lambda - \omega_2) u_\alpha \partial_\alpha n] \\ &\quad + \partial_\alpha [(-\zeta - \omega_1) u_\alpha \partial_\beta n], \end{aligned} \tag{A9}$$

where ν and λ are defined in Eq. (9) and $\zeta = 2\nu - \lambda$.

Equation (A9) shows that it is not possible to choose ω_1 and ω_2 so that the momentum equation is fully Galilean invariant. This occurs because the second moment of f^0, Eq. (6), is symmetric with respect to interchange of its indices, but the viscosity terms do not have this symmetry. To improve the behavior when Galilean invariance is important a sensible choice is

$$\omega_1 = -\zeta, \ \omega_2 = \lambda. \tag{A10}$$

APPENDIX B

Here we present the steps involved in obtaining the equations of motion (32)–(34) from the lattice Boltzmann scheme defined by Eqs. (23) and (24). The derivation of the continuity equation (32) and the Navier-Stokes equation (33) follows that for the one-component fluid presented in Appendix A.

To obtain the convection-diffusion equation (34) we start from the equation analogous to (3) for the distribution functions $\{g_i\}$ describing the density difference. Summing over i and using (26) and (28) gives

$$\begin{aligned} 0 &= \partial_t \Delta n + \partial_\alpha \sum_i g_i^0 e_{i\alpha} - (\tau - \tfrac{1}{2}) \Delta t \\ &\quad \times \left\{ \partial_t^2 \Delta n + 2 \partial_\alpha \partial_t \sum_i g_i^0 e_{i\alpha} + \partial_\alpha \partial_\beta \sum_i g_i^0 e_{i\alpha} e_{i\beta} \right\} \\ &\quad + O((\Delta t)^2). \end{aligned} \tag{B1}$$

It follows immediately from the first two terms on the right-hand side of this equation that

$$\partial_t \Delta n = -\partial_\alpha \sum_i g_i^0 e_{i\alpha} + O(\Delta t). \tag{B2}$$

Using Eq. (B2) shows that the first, together with half of the second, term in curly brackets in Eq. (B1) is of higher order and can be neglected. To simplify the remainder of this equation we shall use

$$\sum_i g_i^0 e_{i\alpha} = \Delta n u_\alpha = \frac{\Delta n}{n} \sum_i f_i^0 e_{i\alpha}, \tag{B3}$$

where the second equality follows from Eq. (25). This is tantamount to assuming that each component is moving with the mean fluid velocity $\vec{u}$. We consider each of the remaining terms in (B1) in turn.

(i) Using Eq. (B3)

$$\partial_\alpha \sum_i g_i^0 e_{i\alpha} = \partial_\alpha (\Delta n u_\alpha). \tag{B4}$$

(ii) Similarly,

$$\partial_\alpha \partial_t \sum_i g_i^0 e_{i\alpha} = \partial_\alpha \partial_t \left(\frac{\Delta n}{n} n u_\alpha \right). \tag{B5}$$

Differentiating each term in the product and replacing the time derivatives by space derivatives using Eqs. (A3), (A4), and (B2) this term gives a contribution

$$-\partial_\alpha\left\{\partial_\beta(\Delta n u_\beta)u_\alpha+(\partial_\beta u_\alpha)\Delta n u_\beta+\frac{\Delta n}{n}\partial_\beta P_{\beta\alpha}\right\}, \tag{B6}$$

where we have used the definition (29) to rewrite the second moment of f_i^0 in terms of the pressure tensor.

(iii) Using the definition (31)

$$\partial_\alpha\partial_\beta\sum_i g_i^0 e_{i\alpha}e_{i\beta}=\partial_\alpha\partial_\beta\{\Gamma\Delta\mu\delta_{\alpha\beta}+\Delta n u_\alpha u_\beta\}. \tag{B7}$$

Substituting (B4), (B6), and (B7) back into (B1) and noting that the first two terms in (B6) cancel with the last term in (B7) gives the convection-diffusion equation (34).

[1] R. Benzi, S. Succi, and M. Vergassola, Phys. Rep. **222**, 145 (1992).

[2] D.H. Rothman and S. Zaleski, Rev. Mod. Phys. **66**, 1417 (1994).

[3] U. Frish, B. Hasslacher, and Y. Pomeau, Phys. Rev. Lett. **56**, 1505 (1986).

[4] F.J. Higuera, S. Succi, and R. Benzi, Europhys. Lett. **9**, 345 (1989).

[5] I. Ginzbourg and D. d'Humières (unpublished).

[6] W.R. Osborn, E. Orlandini, M.R. Swift, J.M. Yeomans, and J.R. Banavar, Phys. Rev. Lett. **75**, 4031 (1995).

[7] F.J. Alexander, S. Chen and D.W. Grunau, Phys. Rev. B **48**, R634 (1993).

[8] S.Y. Chen and T. Lookman, J. Stat. Phys. **81**, 223 (1995).

[9] A.K. Gunstensen and D.H. Rothman, J. Geophys. Res. Solid Earth **98**, 6431 (1993).

[10] A.K. Gunstensen, D.H. Rothman, S. Zaleski, and G. Zannetti, Phys. Rev. A **43**, 4320 (1991).

[11] X.W. Shan and H.D. Chen, Phys. Rev. E **47**, 1815 (1993).

[12] X.W. Shan and H.D. Chen, Phys. Rev. E **49**, 2941 (1994)

[13] X.W. Shan and G. Doolen, J. Stat. Phys. **81**, 379 (1995).

[14] J.S. Rowlinson and B. Widom, *Molecular Theory of Capillarity* (Clarendon, Oxford, 1982).

[15] R. Evans, Adv. Phys. **28**, 143 (1979).

[16] J.W. Cahn and J.E. Hilliard, J. Chem. Phys. **28**, 258 (1958).

[17] A.J. Bray, Adv. Phys. **43**, 357 (1994).

[18] P.L. Bhatnagar, E.P. Gross, and M. Krook, Phys. Rev. **94**, 511 (1954); H.D. Chen, S.Y. Chen, and W.H. Matthaeus, Phys. Rev. A **45**, R5339 (1992); Y.H. Qian, D. d'Humières, and P. Lallemand, Europhys. Lett. **17**, 479 (1992).

[19] M.R. Swift, W.R. Osborn, and J.M. Yeomans, Phys. Rev. Lett. **75**, 830 (1995).

[20] M. De Menech, Laurea thesis, University of Padva, 1996.

[21] W.-J. Ma, P. Keblinski, A. Maritan, J. Koplik and J.R. Banavar, Phys. Rev. Lett. **71**, 3465 (1993).

[22] E. Orlandini, M.R. Swift, and J.M. Yeomans, Europhys. Lett. **32**, 463 (1995).

[23] L.E. Reichl, *A Modern Course in Statistical Physics* (Arnold, London, 1980).

[24] D. d'Humières (private communication).

[25] D.H. Rothman and J.M. Keller, J. Stat. Phys. **52**, 1119 (1988).

[26] C. Appert, J.F. Olson, D.H. Rothman, and S. Zaleski, J. Stat. Phys. **81**, 181 (1995).

[27] U. D'Ortona, D. Salin, M. Cieplak, R.B. Rybka, and J.R. Banavar, Phys. Rev. E **51**, 3718 (1995).

[28] E.G. Flekkøy, Phys. Rev. E **47**, 4247 (1993).

[29] F.J. Alexander, S. Chen, and J.D. Sterling, Phys. Rev. E **47**, R2249 (1993).

[30] M.G. Ancona, J. Comput. Phys. **115**, 107 (1994).

[31] B.T. Nadiga and S. Zaleski (unpublished).